J Plant Growth Regul (2007) 26:329–340
DOI 10.1007/s00344-007-9019-2

Cloning and Biochemical Characterization of *ToFZY*, a Tomato Gene Encoding a Flavin Monooxygenase Involved in a Tryptophan-dependent Auxin Biosynthesis Pathway

Marino Expósito-Rodríguez · Andrés A. Borges · Andrés Borges-Pérez · Mercedes Hernández · José A. Pérez

Received: 2 January 2007 / Accepted: 10 April 2007 / Published online: 20 October 2007

Abstract Indole-3-acetic acid (IAA), the main endogenous auxin, has been known for decades to be a key regulator for plant growth and development. Multiple routes have been proposed for IAA biosynthesis but physiologic roles or relevance of the different routes are still unclear. Recently, four members of the *Arabidopsis thaliana YUC* gene family have been implicated in an additional requirement of IAA involved in floral organ and vascular tissue formation. The loss-of-function *yuc1yuc4* double mutants in *Arabidopsis* displayed phenotypes similar to the previously described loss-of-function *floozy* mutants in petunia (*fzy*). Moreover, it has been demonstrated that *YUC1* encodes a flavin monooxygenase (FMO) that catalyzes a rate-limiting step of a tryptophan-dependent auxin biosynthesis pathway: the conversion of tryptamine to N-hydroxyl-tryptamine. Here we report on the genetic study of *ToFZY*, the putative tomato ortholog of *YUC4* and *FZY*, including gene and cDNA sequence comparison and a preliminary expression analysis. In addition, we describe a novel conserved amino acid motif that may be considered a hallmark potentially useful for the identification of new YUC-like FMOs. We also demonstrate that *ToFZY* encodes a protein with the same enzymatic activity as YUC1. Finally, we provide evidence suggesting that the *ToFZY* gene belongs to a multigenic family whose members may exhibit a temporal and spatial specialization similar to that described in *A. thaliana*.

Keywords Tomato · Flavin monooxygenase-like proteins · Tryptophan-dependent auxin biosynthesis · Tryptamine pathway

M. Expósito-Rodríguez · A. A. Borges (✉) · A. Borges-Pérez · M. Hernández
Instituto de Productos Naturales y Agrobiología – CSIC, Avda Astrofísico Francisco Sánchez 3, P.O. Box 195, 38206 La Laguna, Tenerife, Canary Islands, Spain
e-mail: aborges@ipna.csic.es

M. Expósito-Rodríguez · J. A. Pérez
Departamento de Parasitología, Ecología y Genética – Facultad de Biología, Universidad de La Laguna, Avda, Astrofísico Francisco Sánchez s/n, 38271 La Laguna, Tenerife, Canary Islands, Spain

Introduction

Indole-3-acetic acid (IAA) is the main endogenous auxin, an essential plant hormone that has been implicated in the regulation of many aspects of plant growth and development such as cell division and elongation, apical dominance, vascular differentiation, lateral root production, phototropism, root gravitropism, senescence, abscission, and flowering (Woodward and Bartel 2005).

Multiple routes have been proposed for IAA biosynthesis, including tryptophan-dependent (TD) and tryptophan-independent (TI) pathways, but none of them is completely defined in regard to genes, enzymes, and intermediates, and the control, physiologic role, or the relevance of the different routes are still not fully understood (Bartel and others 2001; Ljung and others 2002; Woodward and Bartel 2005). Zhao and others (2001) have characterized a dominant gain-of-function *Arabidopsis* mutant, named *yucca*, which contains high levels of free auxin. Accordingly, *yucca* seedlings have long hypocotyls, epinastic cotyledons, and elongated petioles, all phenotypes characteristic of auxin overproduction. *YUCCA* gene (*YUC1*) encodes an enzyme with flavin monooxygenase (FMO) activity that is able to catalyze the hydroxylation of the amino group of tryptamine, a rate-

limiting step in one TD IAA biosynthesis pathway (Zhao and others 2001). Shortly after the Zhao report, a gene named *FLOOZY* (*FZY*) was isolated and characterized in petunia by Tobeña-Santamaria and others (2002) and it was proposed as the ortholog of *YUC1*, *YUC2*, and *YUC4*. The loss-of-function *floozy* mutants revealed that the *FZY* gene product is required for floral organ initiation and specification of the vascularization pattern in leaves. Furthermore, overexpression of *FZY* results in increased auxin levels and a phenotype similar to *yucca* plants.

The *YUC* gene family represents one of the two gene families that encode plant FMO-like proteins (the *YUC*-like FMO family) and includes at least 11 paralogs in the *Arabidopsis* genome (Zhao and others 2002). Recently, the functional redundancy in the *YUC* family has been partially defined and it has been demonstrated that like the petunia *FZY* gene, some *YUC* genes spatially and temporally regulate the biosynthesis of an auxin supplement needed for the formation of floral organs and vascular tissues (Cheng and others 2006).

Our research group is currently studying the molecular processes underlying auxin biosynthesis, flower development, and fruit ripening, using *Lycopersicon esculentum* as a model organism because of the worldwide economic relevance of tomato crops. Here we report on the genetic characterization of *ToFZY*, the putative tomato orthologous gene of *FZY* and *YUC4*, and the biochemical confirmation of the flavin-monooxygenase activity supported by the encoded protein. In addition, a new fingerprint for the YUC-like FMO family is proposed. Also, we present evidence pointing out that the tomato genome contains several genes that encode FMO-like proteins, a situation that apparently reflects a functional specialization similar to that proposed for *A. thaliana YUC* genes.

Material and Methods

Growth and Maintenance of Plants

Tomato (*Lycopersicon esculentum*) cv. ciliegia plants were maintained under growth chamber conditions at 25 ± 2°C in standard potting compost in 9-cm-diameter pots (average of two seeds sown per pot). The relative humidity was kept around 60% with a 12-h photoperiod (120 μmol PAR m^{-2} s^{-1}).

Nucleic Acids Isolation

Plant genomic DNA was isolated from young leaves (100 mg) of *L. esculentum* cv. ciliegia using the GenElute™ Plant Genomic DNA Miniprep Kit (Sigma-Aldrich, St. Louis, MO, USA). Total RNA was extracted from plant tissue samples (100 mg), representing different developmental stages, using the Spectrum™ Plant Total RNA Kit (Sigma-Aldrich). RNA was further purified by digestion with DNase I Amplification Grade (Sigma-Aldrich) according to the manufacturer's instructions. RNA integrity was checked by electrophoresis on a denaturing agarose gel and quantified using an Eppendorf biophotometer (Hamburg, Germany). Plasmid cTOF-1-I23 was isolated from bacteria using the GenElute™ Plasmid Miniprep Kit (Sigma-Aldrich).

DNA Amplification by Standard Polymerase Chain Reaction (PCR)

Amplification reactions were performed in a volume of 50 μl containing 50 ng of genomic DNA, 2.5 units of a Hot-Start Taq DNA polymerase blend (JumpStart™ AccuTaq™ LA DNA polymerase; Sigma-Aldrich), 1 × reaction buffer (50 mM Tris-HCl; 15 mM $(NH_4)_2SO_4$, pH 9.3; 0.001% Tween-20; 2.5 mM $MgCl_2$), 200 μM of each dNTP, and 1 μM of each primer (Table 1). Reactions were incubated in the Applied Biosystems 2700 thermocycler (Foster City, CA, USA) using the following temperature profile: initial denaturing at 96°C for 10 s, followed by 35 amplification cycles of denaturing at 94°C for 10 s, optimized annealing temperature (Table 1) for 20 s, and extension at 72°C for 30 s, with a final extension step at 72°C for 5 min. The amplified DNA fragments were separated by electrophoresis on 1.5% agarose gels in TBE buffer and visualized after ethidium bromide staining.

Degenerate Oligonucleotide Primed-PCR (DOP-PCR)

A pair of degenerate primers were used in the DOP-PCR strategy (Table 1) with genomic DNA as template. Amplification reactions were carried out using the reactive concentrations and final volume given above, except for oligonucleotide p1L, which was used at 10 μM to compensate for its high degeneration level. The DOP-PCR thermal profile was as follows: initial denaturing step at 96°C for 10 s, followed by 35 amplification cycles of denaturing at 94°C for 10 s, annealing temperature for 30 s, and extension at 72°C for 5 s, with a final extension step at 72°C for 1 min. During the first 15 amplification cycles the annealing temperature was lowered from 65°C to 51°C at 1°C/cycle rate, and maintained at 50°C for the last 25 cycles.

Inverse PCR

A genomic DNA sample (500 ng) was digested with 10 units of a single restriction enzyme (*Nde*II or *Taq*I) in a

Table 1 Oligonucleotides used as primers in the amplification reactions

	Name	Sequence (5′→3′)	Target site on *ToFZY* gene	Orientation	T_a
Standard PCR	I5a	GACATAACGCCATTCCTCATA	Exon I	Sense	62
	III1b	CAAGAAGGCACATTGCTTTTG	Exon III	Antisense	
	III1a	AATGCCAGGTGTGAAGGAAAT	Exon III	Sense	
	3U-1b	TGTAGTAGCAGAGCCACCAATA	3'-UTR	Antisense	
	F-*Nco*I	TGGTGCCGCCATGGGTTGTTGTAAAGAGGAAG	Exon I (start codon)	Sense	68
	R-*Bgl*II	TCGTGGGGAGATCTAAAACATATGCCTTGGTTATCTG	Exon IV (stop codon)	Antisense	
DOP-PCR	p1L	GGNGCNGGNCCNWSNGGNYTNGC	Exon I	Sense	Touch-down (see text)
	p1R	CATNCCNSWRTTNCCRCANCC	Exon I	Antisense	
Inverse-PCR	I3a	AATACCCCACAAAACACCAGTTCAT	Exon I	Sense	65
	I3b	CGGGAGTTGACAGAATTGTTTAGG	Exon I	Antisense	
RT-PCR	2a	TGGATGCCTTTAAGAATAGTTG	Exon II	Sense	58
	3b	TGTATCCTGTTGCTAAGATTATTG	Exon III	Antisense	
	EF-1αa	CTCAGGCTGACTGTGCTGTTC	—	Sense	
	EF-1αb	ACAGGGACAGTTCCAATACCAC	—	Antisense	

T_a = optimized annealing temperature

The following code was used for degenerated primers: N (any nucleotide); R (A or G); S (C or G); W (A or T); Y (C or T)

volume of 20 µl and incubated at 37°C for more than 20 h to ensure completed digestion. Restriction fragments ranging from 10 kb to 100 bp were purified with the GenElute™ PCR Clean-Up Kit (Sigma-Aldrich). Subsequently, circular molecules were obtained by self-ligation of restriction fragments (3 ng/µl) with T4 DNA ligase (DNA Ligation Kit ver. 2.1; Takara Bio Inc., Japan) following the manufacturer's recommendations. Circularized DNA molecules (4 µl of the ligation reaction) were utilized as a template for inverse PCR using a pair of divergent primers (Table 1) and the standard reaction conditions (see above), with the following temperature profile: initial denaturing at 96°C for 10 s, followed by 35 amplification cycles of denaturing at 94°C for 10 s, annealing at 65°C for 15 s, and extension at 68°C for 10 min, with a final extension step at 68°C for 15 min.

Reverse Transcription PCR (RT-PCR)

First-strand cDNA synthesis was accomplished with specific primers for *ToFZY* and elongation factor-α1 (*EF*-α1) mRNAs (Table 1) in a multiplex format and application of a thermal ramp during the annealing step. Reaction mix (20 µl) included total RNA (1.5 µg), primers (1 µM each one), dNTP mix (500 µM each one), RNase inhibitor (20 units; Sigma-Aldrich), and reaction buffer 1 × (Sigma-Aldrich). To perform primer annealing the reaction mix was heated at 70°C for 10 min and then the temperature was gradually dropped to 41°C at a 1°C/30 s rate. Finally, the reaction was incubated at 37°C with 200 units of M-MLV reverse transcriptase (Sigma-Aldrich) for 50 min and stopped by heating at 94°C for 10 min.

cDNA amplifications were carried out in the standard PCR conditions (see above) using 2 µl of cDNA template and in separated reactions for *EF*-α1 and *ToFZY*. Cycle numbers were optimized to ensure that amplification of both *EF*-α1 and *ToFZY* remained in the exponential amplification range. Thermocycling conditions were as follows: initial denaturing at 96°C for 10 s, followed by 25 (*EF*-α1) or 30 (*ToFZY*) amplification cycles of denaturing at 94°C for 15 s, annealing at 58°C for 15 s, and extension at 72°C for 30 s, with a final extension step at 72 °C for 5 min. The results of RT-PCR were checked by electrophoresis on agarose gel.

DNA Sequencing and Bioinformatic Tools

DNA templates for sequencing reactions were PCR products purified with the GenElute™ PCR Clean-Up Kit (Sigma-Aldrich) or the plasmid cTOF-1-I23. Both strands were completely sequenced using M13 universal primers with the plasmid template, amplification primers with PCR templates, or internal primers with both types of templates. Sequencing reactions were carried out with a BigDye® Terminator v3.1 Cycle Sequencing Kit according to manufacturer's instructions (Applied Biosystems), except for degenerate primer p1R, which was used at a concentration sevenfold higher than recommended. The sequencing

reaction products were separated, after ethanol precipitation, on an ABI PRISM 3700 automated DNA sequencer (Applied Biosystems). Partial sequences were assembled with the SeqEd ver. 1.03 program (Hageman and Kwan 1997).

Primers for PCR or sequencing were designed with GeneRunner 3.05 (Hastings Software Inc., Hastings-on-Hudson, NY, USA). Nucleotide or amino acid sequence alignments and phylogenetic analyses were performed with MEGA ver. 3.1 (Kumar and others 2004). Database searches for sequence identities were carried out with the BLAST application available from the NCBI and the SOL Genomics Network (Cornell University; http://www.sgn.cornell.edu).

Expression of Recombinant ToFZY Protein in *Escherichia coli*

With the intention of expressing ToFZY in *E. coli* as a C-terminal 6 × His-tagged protein, the complete coding DNA sequence of the *ToFZY* gene was amplified by PCR and subcloned in the plasmid vector pQE-60 (Qiagen, Valencia, CA, USA). For this purpose, PCR was carried out with the tailed primers F-*Nco*I and R-*Bgl*II (Table 1) that incorporated the appropriate restriction sites at the ends of the amplicon, and using as DNA template the plasmid cTOF-1-I23 (Tomato EST Distribution Center, USDA Plant, Soil and Nutrition Laboratory), which harbored a cDNA-encoding ToFZY protein. Two factors helped to minimize the generation of mutated DNA fragments in the standard amplification reaction (see above): (1) JumpStart™ AccuTaq™ LA DNA polymerase has a higher fidelity (up to 6.5-fold) than the standard, and (2) the plasmid template was adjusted to 20 ng to recover enough amplicon with only ten PCR cycles. The amplification product (1254 bp) was electrophoresed and gel purified with the GenElute™ PCR Clean-Up Kit (Sigma-Aldrich) to avoid plasmid contamination. After double digestion with *Nco*I/*Bgl*II and ligation to the pQE-60 vector, the recombinant construct (pQE-60-*ToFZY*) was transformed into *E. coli* M15[pREP4] (Qiagen). The absence of new mutations in three selected clones was checked by sequencing.

A single *E. coli* clone harboring pQE-60-*ToFZY* was grown overnight in 10 ml of LB media with 25 µl/ml kanamycin and 100 µl/ml ampicillin (pREP4 and pEQ-60 selection, respectively). Preculture was added to 250 ml of fresh LB medium with antibiotics and incubated at 30°C with vigorous shaking until OD_{600} reached 0.5–0.7. *ToFZY* cDNA expression was induced with 0.6 mM isopropyl-β-D-thiogalactopyranoside (IPTG) in the presence of 50 µM FAD. After a 4-h induction, the cells were harvested by centrifugation at 4500*g* for 30 min at 4°C, washed with cold potassium phosphate buffer (50 mM, pH 8.5), and stored at –20°C. The adequate production of recombinant protein was verified through SDS-PAGE (Laemmli 1970): 1 ml of induced cells was taken from cultures, pelleted (16,000*g*, 5 min), resuspended in 1 × loading buffer (100 µl), boiled for 10 min, and centrifuged at 13,000*g* for 10 min; the cleared lysate (30 µl) was directly loaded on a denaturing polyacrylamide gel. A suitable control (bacteria transformed with pQE-60 vector) was processed in parallel following exactly the same protocol.

Chemical Synthesis of *N*-hydroxyl-tryptamine

An *N*-hydroxyl-tryptamine standard was obtained by chemical synthesis in two reaction steps. First, 3-(2-nitroethyl)-indole was synthesized as described by Hermkens and others (1990). Sodium methoxide (54 mg, 1 mmol) was added to a 5 ml of stirred solution of gramine (174 mg, 1 mmol) and dimethyl sulfate (0.1 ml, 1 mmol) in nitromethane/methanol (2/1). After completion of the reaction (24 h), monitored by TLC ($CHCl_3$:MeOH, 99:1 v/v), most of the solvent was removed by evaporation *in vacuo* at room temperature. The residue was dissolved in dichloromethane and subsequently washed with 5% NH_4OH, 1 N HCl, and brine. The organic layer was dried over Na_2SO_4 and the solvent was evaporated *in vacuo*. The residue was purified by chromatography in a silica-phase column ($CHCl_3$:MeOH, 99:1 v/v) to yield 150 mg of 3-(2-nitroethyl)-indole. The molecular structure of this product was confirmed by ^{1}H-NMR [(CDCl3, 400 MHz) dH 8.03 (1H, bs, NH), 7.54 (1H, d, J = 7.9 Hz, Ar-H), 7.32 (1H, d, J = 7.9 Hz, Ar-H), 7.21 (1H, t, J = 7.9 Hz, Ar-H), 7.14 (1H, t, J = 7.9 Hz, Ar-H), 6.97 (1H, d, J = 1.2 Hz, 2-H), 4.62 (2H, t, J = 7.2 Hz, N-CH2), 3.44 (2H, t, J = 7.2 Hz, CH2)].

The reduction of the nitro group from 3-(2-nitroethyl)-indole to yield *N*-hydroxyl-tryptamine was carried out as described by Yamada and others (1998). Zinc powder (50 mg, 0.75 mmol) was added in small portions to a stirred solution of 3-(2-nitroethyl)-indole (25 mg, 0.13 mmol) and NH_4Cl (14 mg, 0.26 mmol) in tetrahydrofuran (1 ml) and H_2O (0.5 ml) at room temperature over a period of 10 min. After stirring at room temperature for 20 min, the mixture was filtered through a Celite pad. The organic layer was separated, washed with brine (10 ml), and dried over Na_2SO_4. Evaporation of the solvent gave crude *N*-hydroxyl-tryptamine as a yellow solid. The molecular structure of the final reaction product was verified by both ^{1}H-NMR [($CDCl_3$, 400 MHz) δ_H 8.11 (1H, bs, NH), 7.60 (1H, d, J = 7.9 Hz, Ar–H), 7.33 (1H, d, J = 7.9 Hz, Ar–H), 7.18 (1H, t, J = 7.9 Hz, Ar–H), 7.11 (1H, t, J = 7.9 Hz, Ar–H),

6.98 (1H, d, J = 1.2 Hz, 2–H), 4.45 (2H, bs), 3.23 (2H, t, J = 7.2 Hz, N–CH_2), 3.01 (2H, t, J = 7.2 Hz, CH_2)] and mass spectrometry [(EI) m/z (relative intensity) 174 (M^+, 27), 158 (11), 144 (23), 130 (M^+–CH_2NHOH, 100), 117 (11)].

Activity Assay of Recombinant ToFZY Protein

Enzymatic conversion of tryptamine to *N*-hydroxyl-tryptamine was assayed on *E. coli* lysates from cells expressing recombinant *ToFZY* cDNA or bacteria transformed with the empty expression vector (negative control). Cells expressing recombinant ToFZY protein (see above) were frozen/thawed, resuspended in 5 ml of cold potassium phosphate (50 mM, pH 8.5), and disrupted by sonication using a microtip probe. Because FMO-like proteins show a considerable thermal lability (Cashman 2002), sonication pulses were short (10 s separated by 1-min intervals) and the system was maintained on ice all the time to preserve enzymatic activity. After centrifugation at 16,000*g* for 30 min at 4°C, a 30-µl supernatant sample was electrophoresed in denaturing conditions for monitoring the efficiency of cell disruption and the level of soluble recombinant ToFZY. The remaining soluble phase was recovered and dialyzed three times for 1 h at 4°C against 1 L of cold potassium phosphate (50 mM, pH 8.5) and 50 µM FAD in a dialysis bag with an exclusion limit of 12 kDa.

Enzymatic activity was assayed in a mix reaction (1 ml) containing 50 µl of protein extract, 10 mM tryptamine, 1 mM $NADP^+$, 1 mM glucose-6-phosphate, 2 units of glucose-6-phosphate dehydrogenase, and 50 µM FAD. After incubation at 37°C for 3 h, tryptamine remains or the reaction product were extracted four times with diethylic ether (4 ml). The four organic phases were pooled, dried over Na_2SO_4, and evaporated *in vacuo* and the residue was dissolved in 3.5 ml of methanol. Aliquots (20 µl) of the methanolic solution were analyzed on a Beckman-Coulter 125P HPLC system with UV detection (photodiode model 168), fitted with a 5-µm Beckman Ultrasphere ODS reverse-phase column (4.6 mm × 15 cm) with a mobile phase of acetonitrile:H_2O (8:2 v/v).

Results

Sequencing of *ToFZY* Gene and mRNA

The entire sequence of the *ToFZY* gene was inferred by assembling partial DNA sequences from overlapped amplicons obtained by different PCR strategies. First, degenerate oligonucleotides p1L and p1R (Table 1) were designed on consensus amino acid sequences that include the FAD and NADPH binding motifs, a feature of many FAD-containing enzymes (Dym and Eisenberg 2001). The two amino acid stretches that preferentially configure these conserved motifs in plant FMO-like proteins of the YUC family (Figure 1A) were defined after the multiple alignment of the FZY protein from *Petunia hybrida* (AAK74069), the YUC1 (NP_194980) and YUC4 (NP_196693) proteins from *Arabidopsis thaliana*, and other related amino acid sequences from *Medicago truncatula* (ABE92660) and *Oryza sativa* (NP_917203). DOP-PCR with primers p1L/p1R and genomic DNA template from *L. esculentum* cv. ciliegia yielded a predominant electrophoresis band (Figure 1B) with the expected size (501–508 bp). This band was recovered from the electrophoresis gel and sequenced with the same amplification primers without prior cloning in bacteria. Surprisingly, although the DOP-PCR approach was intended to identify any member of a putative tomato *YUC* gene family, sequencing electropherograms were perfectly legible, indicating that the selected DNA band corresponded to a homogeneous PCR product that probably originated from a single locus. This may reflect a competition effect due to highly restrictive conditions during the annealing step that favored a single amplicon. Nevertheless, the deduced tomato sequence (507 bp) showed a 99.8% identity with a portion of *FZY* exon I, indicating that we had obtained a partial sequence from a tomato gene homologous to petunia *FZY*. This DNA sequence allowed the divergent primers I3a and I3b to be designed (Table 1) and then used in an inverse-PCR approach. In this regard, two different restriction endonucleases were assayed separately and the two main amplicons were sequenced with internal primers (Figure 1C). The combination of DOP-PCR and inverse-PCR strategies allowed us to assemble a 1302-bp contig (Figure 1D), which included a segment upstream from the start codon (580 bp), exon I coding sequence, and a segment from intron I (95 bp).

A database search for tomato DNA sequences similar to our partial genomic sequence led us to an expressed sequence tag (EST4688332, 5′ partial sequence; Sol Genomics Network), which was provided to us by the Tomato EST Distribution Center (USDA Plant, Soil, and Nutrition Laboratory) as a plasmid clone named cTOF-1-I23. The complete sequence of this full-length cDNA (1646 bp without poly-A tail) was deduced and deposited in GenBank under accession number AM177499. These new sequence data were used for the molecular cloning of the 3′ half of *ToFZY* gene as two overlapping amplicons obtained by standard PCR with the primer pairs I5a/III1b and III1a/3U1b (Table 1). The sequence of these two DNA fragments was established (687 bp and 1336 bp, respectively) and incorporated into the previous contig (Figure 1D). Finally, the 3078-bp DNA sequence containing the *ToFZY*

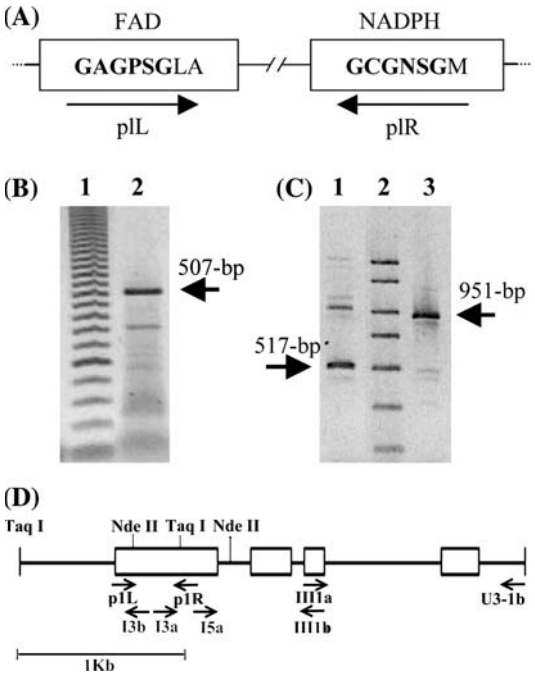

Fig. 1 PCR-based cloning of different segments of the *ToFZY* gene. **A** Consensus amino acid sequences used to design degenerate primers p1L and p1R. Putative FAD and NADPH binding motifs (highlighted in bold) are located near the amino terminus and in the middle of the plant FMO-like proteins, respectively. **B** DOP-PCR with primers p1L and p1R. Arrow points to the amplicon with the expected size. Lane 1: *50-bp ladder* from Amersham-Pharmacia. **C** Inverse-PCR with primers I3a and I3b. Arrows point to the sequenced DNA fragments. Lane 1: DNA template digested with *Nde*II. Lane 2: *PCR marker* from Sigma-Aldrich. Lane 3: DNA template digested with *Taq*I. **D** Relative positions of the target sites for primers used in the PCR contig construction

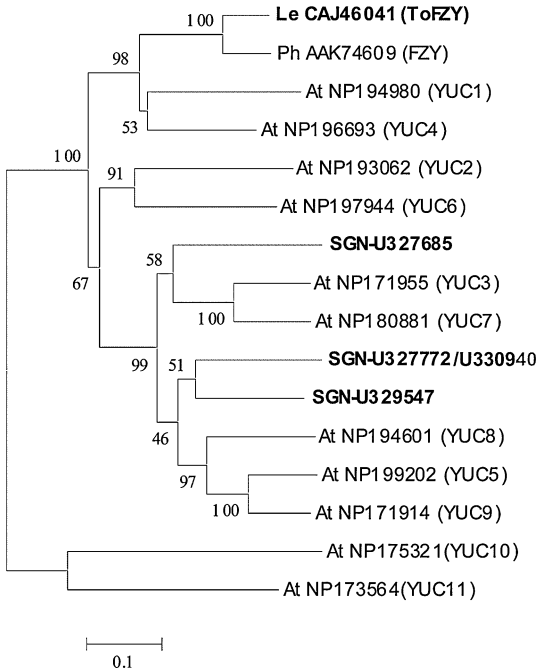

Fig. 2 Neighbor-joining tree showing the phylogenetic relationships among *Arabidopsis* YUC proteins, petunia FZY, ToFZY, and related tomato amino acid sequences. YUC10 and YUC11, the most divergent *Arabidopsis* YUC proteins, were used as an outgroup. Tomato sequences are highlighted in bold. The bootstrap values (1000 replicates) are indicated near the nodes. The scale indicates the number of amino acid substitutions per site. At: *A. thaliana*;. Le: *L. esculentum*; Ph: *P. hybrida*; SGN, UniGene accession numbers from the Tomato International Sequencing Project

gene was deposited in the GenBank under accession number AM177498.

Sequence Analysis of *ToFZY* and Other YUC-like FMOs

Sequence analysis of the *ToFZY* cDNA showed that it encodes a 410-amino-acid protein (GenBank accession No. CAJ46041) that contains a conserved binding motif for FAD and NADPH. *ToFZY* shares a 87, 70, and 69% amino acid sequence identity with FZY, YUC4, and YUC1 proteins, respectively. A neighbor-joining analysis indicated that the four mentioned proteins are grouped in one clade supported by a high bootstrap value (Figure 2), and it also showed that the tomato and petunia proteins are more phylogenetically related to YUC4 protein than to YUC1. Comparison of *ToFZY* cDNA and gene sequences revealed that its coding sequence is interrupted by three introns in exactly the same position as the three introns in *FZY*, *YUC1*, and *YUC4* genes. Interestingly, the sizes of *ToFZY* introns (data not available for *FZY* gene) are more similar to *YUC4* introns than to those from *YUC1*. Taken together these findings indicate that *ToFZY* is the tomato ortholog of petunia *FZY* and *Arabidopsis YUC4*.

In addition to FAD and NADPH binding motifs, two other conserved amino acid sequences that are present in ToFZY reinforce the inclusion of this protein in the YUC-like FMO family. On the one hand, there is a DX_3(L/F)ATGY$(X)_4$P-motif located in the C-terminal part of FAD/NADPH-dependent enzymes with *N*-hydroxylating activity from mammals (FMOs), yeast, fungi, and bacteria (Stehr and others 1998). This conserved motif might be defined more accurately for most sequences that belong to the YUC family (Figure 3): DX(I/V)(I/V)(L/F)ATGY(K/R)SNVP. On the other hand, there is a WL(I/V)VATGENAE motif, first described in this study, located between the FAD and NADPH binding motif which seems to be exclusive of plant FMO-like proteins (at least it is not present in mammalian FMOs) and particularly conserved in the YUC family (Figure 3). We suggest that both hallmarks, especially WL(I/V)VATGENAE, may be potentially useful for the identification of new YUC-like FMOs, although some variance is expected for members of the YUC10/YUC11 clade (Figures 2, 3).

Enzymatic Activity of ToFZY Protein

To confirm whether ToFZY protein has the same enzymatic capability as YUC1, that is, the conversion of tryptamine to *N*-hydroxyl-tryptamine (NHT), we expressed ToFZY in *E. coli* as a C-terminal 6 × His-tagged protein (Figure 4A). However, the recombinant ToFZY produced in *E. coli* had a molecular weight (40.6 kDa) lower than that deduced from the complete amino acid sequence of the fusion protein (46.6 kDa). This difference in size may be explained by the loss of 45 amino acids from the C-terminal end, probably due to two adjacent arginine codons (AGA) that are used in *E. coli* at very low frequency. This hypothesis is supported by the fact that we were unable to purify the heterologous protein by chromatography through a nickel-nitrilotriacetic acid matrix (Qiagen), indicating the possible lack of the C-terminal affinity tag. A similar assay with a C-terminal-truncated yeast FMO (lack of 38 amino acids) demonstrated that it retained its enzymatic activity although with a weak retention of FAD (Suh and others 1996; Zhang and others 2002). Thus, we decided to detect FMO activity on crude *E. coli* extracts and to incorporate FAD during expression of ToFZY in *E. coli*, dialysis of protein extracts, and enzymatic assay.

Crude enzyme extracts were assayed for *N*-hydroxylating activity with tryptamine as substrate and using HPLC analysis for the identification of the reaction product. We used as standards commercial tryptamine (Figure 4B.1) and NHT synthesized in our laboratory (Figure 4B.2). After the incubation step, tryptamine was detected only in the control reaction with cell extracts from *E. coli* transformed with the empty expression vector (Figure 4B.3), whereas NHT was recovered only from the reaction carried out with cell extracts from *E. coli* transformed with pQE-60-*ToFZY* (Figure 4B.4). In addition, a peak adjacent to NHT (Figure 4B.4), with a retention time different than that of tryptamine, was found. We suggest that this could be an intermediate of the enzymatic reaction. According to Cashman (2002), NHT is proposed to be *N*-oxygenated a second time to produce the unstable *N*,*N*-dihydroxy intermediate. The highly labile *N*,*N*-dihydroxy intermediate dehydrates to produce the oxime.

Expression of *ToFZY* Gene

Data about expression patterns may provide clues about the role of the *ToFZY* gene during development. In this sense, we carried out a preliminary study of *ToFZY* expression at

CONSENSUS →	WL(I/V)VATGENAE	DX(I/V)(I/V)(L/F)ATGY(K/R)SNVP
Le CAJ46041 (ToFZY)	WLIVATGENAE	DSIILATGYKSNVP
At NP194980 (YUC1)	..........D	....F.....
Ph AAK74609 (FZY)	....	.....
Mt ABE92660	....	.A.....
At NP196693 (YUC4)	..V.....	.....
Os NP917203	..V.....	.T.....R....
Os NP912652	..V..S.....	.AV.F....R....
Os NP471144	..V.....	.AVV.....R....
Os XP477812	..V.....	.AV.....Q....
At NP171955 (YUC3)	.IV.....	..V.....R....
At NP180881 (YUC7)	..V.....	..V.....R....
At NP194601 (YUC8)	..V.....	..VV.....R....
Mt ABE89940	..V.....	.AVV.....R....
At NP171914 (YUC9)	..V.....	.AVV.....R....
At NP199202 (YUC5)	..V.....	.AVV.....R....
Os BAD87432	..V.....	.V.V.....
Os NP916435	..V.....	.V.V.....
Os AAU43964	..V.....S.	.A.V.....
At NP197944 (YUC6)	..VA.....	.A.....
Mt ABE83417	....	.A.....
At NP193062 (YUC2)	..V.....	.A.....
Os ABA99096	..V.....V	.AV.F.....
Os NP913428	..V.....	.VV.....
At NP173564 (YUC11)	FMVA.....G.	...VF.....S.S
At NP175321 (YUC10)	F.V.....GD	.A.VF.....S.C
Zm BT016604	F.V.....C.	..LVF....R.TAN
Os ABA96025	F.V..S...SA	.A.VF....T.TAN
Os BAD28283	F..M....KSA	.A.VF.....T.N
Os ABA92044	F.V.....SA	.A.VF.....T.N
Os XP493785	H.VA.A...D.	.A.VF....R.TTK
Os XP493782	H.VA.A...D.	.AVVF....R.TTK
Os BAD88343	AVV....QYSQ	.AV.YGGEGHRRRQ
Os BAD89476	AVV....HYSQ	.AV.YC...NYSF.
Os BAD54210	AVV..V.SYTQ	.TVVYC...SYSY.
At NP176448	AVV.CN.HYI.	.V.MHC....YHF.
At AAM61259	AVV.CN.HYI.	.V.MHC....YHF.
At NP172684	AVV.CN.HYT.	.T.MHC....YYF.
At NP172678	AVV.CN.HYT.	.T.VHC....YHF.
At NP564797	AVVMCC.HF..	.T.VHC....YYF.
At NP176444	AVV.CN.HYT.	...VYC....Y.F.
At NP176761	AVV.CS.HFT.	.T.VHC....YYF.
At NP564796	AVV.CS.HYT.	...VYC....YRFT
At AAD43611	AVV.CS.HYT.	...VYC....YRFT

Fig. 3 Multiple alignment of two conserved amino acid motifs found in plant FMO-like proteins. Partial sequences from 43 monocots and dicots are included. Consensus sequences are highlighted in bold. The box delimits members of the YUC family. The other partial sequences belong to the second family of plant FMO-like proteins proposed by Zhao and others (2001). At: *A. thaliana*;. Le: *L. esculentum*; Mt: *M. truncatula;* Os: *O. sativa* cv. japonica; Ph: *P. hybrida*; Zm: *Zea mays*

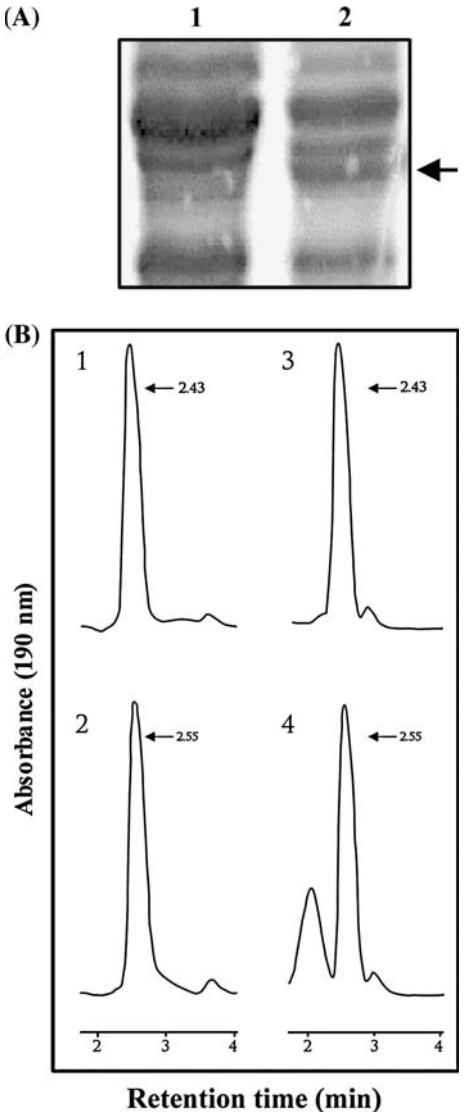

Fig. 4 Expression of *ToFZY* in *E. coli* and FMO activity assay. **A** SDS-PAGE of soluble protein extracts from bacteria induced with IPTG. Lane 1: control cells transformed with the empty expression vector. Lane 2: cells transformed with plasmid pQE-60-*ToFZY*. Arrow points to the recombinant ToFZY protein. **B** HPLC analysis: (1) tryptamine standard, (2) *N*-hydroxyl-tryptamine standard, (3) control reaction, (4) enzymatic reaction with recombinant ToFZY. Arrows indicate the retention time (min) of the corresponding peaks

the transcriptional level using RT-PCR analysis. As shown in Figure 5, the stronger signal is observed in immature flowers, whereas in mature flowers *ToFZY* mRNA reaches an intermediate level between immature flowers and young leaves. Moreover, the significant level of *ToFZY* mRNA observed in young leaves drops dramatically during the maturation process. Finally, expression of *ToFZY* was undetectable in the root apex. Overall, our results on the transcriptional pattern of *ToFZY* were concordant with those reported for the petunia *FZY* gene and *Arabidopsis YUC1/YUC4* genes, especially with *YUC4*. Tobeña-

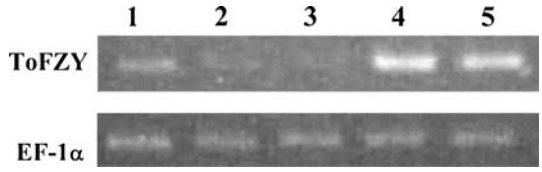

Fig. 5 RT-PCR analysis of *ToFZY* expression in different organs of tomato plants. *ToFZY* and *EF-α1* cDNA fragments were amplified in separate reactions. The *EF-α1* was used as a control for the total RNA input and reverse-transcription step. Lane 1: young leaf; Lane 2: mature leaf; Lane 3: root apex; Lane 4: immature flower; Lane 5: mature flower

Santamaria and others (2002) carried out an *in situ* hybridization analysis of *FZY* mRNA. Although root and mature flower samples were not included, they readily detected the expression of the *FZY* gene in young leaves and immature flowers. In young leaves *FZY* is expressed in a central layer of cells throughout the leaf blade, whereas in older leaves expression is restricted mainly to scattered cells, which may be interpreted as a decrease in the transcription rate of the *FZY* gene in the whole mature leaf. In addition, Cheng and others (2006) studied the expression pattern of *YUC1* and *YUC4* by mRNA *in situ* hybridization and histochemistry analysis of GUS reporter lines. Both genes are expressed in young leaves, although the signal from *YUC4* is weaker and spotted, and both genes are apparently not transcribed in mature leaves. With regard to flowers, *YUC1* is expressed mainly in early developmental stages and completely shut down in mature flowers, whereas *YUC4* transcription is evident in all stages of floral development and in mature flowers. These results of Cheng and others were consistent with the normalized transcription profile data available from the *Arabidopsis* full-genome chip array (Affymetrix ATH1: analysis by AtGenExpress [http://www.web.uni-frankfurt.de/fb15/botanik/mcb/AFGN/atgenex.htm]), which also indicate that *YUC1* and *YUC4* are not expressed in *Arabidopsis* roots.

Search for Putative ToFZY Paralogs

A detailed search for other tomato sequences showing similarity to the ToFZY protein in the Sol Genomics Network database allowed us to identify several cDNA partial sequences that are clustered in four UniGene accessions: SGN-U327685, SGN-U327772, SGN-U330940, and SGN-U329547. In fact, SGN-U327772 and SGN-U330940 represent 5′ and 3′ partial sequences, respectively, from the same cDNA clones and therefore they will be referred to as SGN-U327772/SGN-U330940. The amino acid sequences encoded by these three tomato genes contain several conserved motifs that are considered

Table 2 Conserved amino acid motifs found in the putative ToFZY paralogs

	No. aa	CM1	CM2	CM3	CM4
SGN-U327685	247	—	—	+	+
SGN-U327772	276[a]	+	+	—	+
SGN-U329547	347	—	+	+	+

No. aa = amino acids number; CM = conserved motif; CM1 = FAD binding; CM2 = WL(I/V)VATGENAE; CM3 = NADPH binding; CM4 = DX(I/V)(I/V)(L/F)ATGY(K/R)SNVP; + = present; — = not encompassed by the partial sequences

[a] Separate N-terminal and C-terminal segments

attributes of FMO-like proteins (Stehr and others 1998; Dym and Eisenberg 2001; Cashman 2002). Moreover, two of the three amino acid sequences include the WL(I/V)VATGENAE motif proposed in this study as a distinctive feature of YUC-like FMOs (Table 2). In view of these findings, it appears that *ToFZY* belongs to a *YUC* gene family consisting of at least four paralogs.

The phylogenetic relationships among ToFZY, the three putative tomato YUC-like FMOs (incomplete amino acid sequences) and *Arabidopsis* YUC proteins are shown in Figure 2. None of the three partial amino acid sequences from tomato are grouped with ToFZY. SGN-U327685 appears to encode the ortholog of *Arabidopsis* YUC3/YUC7, whereas proteins encoded by SGN-U327772/SGN-U330940 and SGN-U329547 are closely related and positioned in the same clade as YUC5/YUC8/YUC9.

Discussion

Indole-3-acetic acid (IAA) is the main endogenous auxin in most plants. The possible routes for IAA biosynthesis are classically subdivided into tryptophan-dependent (TD) and tryptophan-independent (TI) pathways, depending on whether they are initiated from tryptophan (Trp) or from an indolic Trp precursor. In addition, some IAA demands may also be fulfilled by β-oxidation of indole-3-butyric acid, a second endogenous auxin, or by hydrolyzing IAA conjugates. The multiple pathways for IAA biosynthesis, as well as the redundancy at the gene level within a single biosynthetic pathway, appear to be a feature of plant genetic resources (Bartel and others 2001; Ljung and others 2002; Cohen and others 2003; Woodward and Bartel 2005).

The widely accepted concept that plants can use several pathways to synthesize IAA can be illustrated with the following example. In *L. esculentum*, apart from the TI pathway for IAA production (Epstein and others 2002), at least two of the four proposed TD pathways (Woodward and Bartel 2005) appear to operate: the tryptamine pathway and the indole-3-pyruvic acid (IPA) pathway. On the one hand, the presence of enzymes capable of converting tryptamine to IAA in tomato shoots and tomato cell-free extracts has been demonstrated (Gibson and others 1972). On the other hand, Cooney and Nonhebel (1991) detected and quantified IPA in tomato shoots, and the amounts of ^{2}H-labeled IPA were quantitatively consistent with a role as a precursor. These researchers also concluded that in tomato shoots the IPA pathway for IAA biosynthesis is quantitatively more important than the tryptamine pathway. With regard to the other possible TD routes, the CYP79B2/B3 pathways (also known as the indole-3-acetonitrile (IAN) pathway; Bartel and others 2001) may be discarded in the Solanaceae family because tobacco apparently lacks genes encoding the cytochromes P450 of the CYP79B subfamily which convert Trp to IAOx (Bak and others 1998). Indeed, the CYP79B2/B3 route seems to be specific for indole-glucosinolate-producing plants and glucosinolates function as a general defense against herbivore attack (Halkier and others 1997).

An increasing body of evidence suggests that the TD and TI pathways differ in their relevance with regard to environmental responses or developmental processes. In general, it appears that TI pathways account for IAA maintenance during normal plant growth, but a switch to TD pathways occurs when high IAA levels are required because the large Trp pool is capable of sustaining a higher biosynthetic rate. For instance, Sztein and others (2002) demonstrated that germinating bean axes preferentially utilize the TI pathway, but after cotyledon excision the TD pathway is induced to supply the high IAA levels required for rapid cell proliferation in wounded tissues. In a similar way, the *CYP79B2* gene is expressed in *Arabidopsis* after wounding (Mikkelsen and others 2000) and in response to infection with a bacterial pathogen (Hull and others 2000), both in coordination with Trp biosynthetic genes. Besides the stress-induced switching of IAA biosynthetic pathways, several cases of developmental regulation have been reported. Epstein and others (2002) detected a change from the TD to the TI pathway that occurs between mature green and red-ripe stages of tomato fruit development, which may be the result of the cessation of cell growth. Early stages of embryogenesis in carrot are characterized by a high input of free IAA derivate from Trp, whereas the basal levels are maintained by a TI pathway (Ribnicky and others 2002). To complete this compilation, the analyses of inactivation-tagging mutants revealed that the petunia *FZY* gene and certain combinations of *Arabidopsis YUC* genes are involved in leaf venation pattern and floral development (Tobeña-Santamaria and others 2002; Cheng and others 2006), and the spatially restricted and temporally controlled activation of these genes may be interpreted as a switch from basal IAA biosynthesis to a particular TD pathway (the tryptamine route). Indeed, the *yuc* (single or

combined) and the *fzy* loss-of-function mutants displayed normal levels of free auxin.

Because the tryptamine pathway for IAA biosynthesis is a central issue of the present study, some considerations about its regulation are worth noting. The first step in the tryptamine pathway for IAA biosynthesis, the conversion of Trp to tryptamine, is catalyzed by Trp decarboxylase (TDC). Transcription of the TDC gene is repressed by IAA (Goddijn and others 1992) in *Catharanthus roseus*. However, overexpression of TDC in tobacco leads to tryptamine accumulation without high auxin phenotypes (Songstad and others 1990), suggesting that TDC does not control the flux through the tryptamine pathway. Interestingly, CYP83B1 is inhibited by tryptamine in *Arabidopsis* (Bak and others 2001), probably avoiding IAOx molecules being channeled to indole-glucosinolate synthesis when free IAA production is required. The second proposed step in the tryptamine pathway is the conversion of tryptamine to *N*-hydroxyl-tryptamine (NHT). This conversion can be catalyzed *in vitro* by the *Arabidopsis* YUC1 protein (Zhao and others 2001) and by the tomato ToFZY protein in the present study. The finding that transgenic plants overexpressing a *YUC* gene accumulate free IAA and display high auxin phenotypes (Zhao and others 2001; Tobeña-Santamaria and others 2002; Woodward and others 2005; Cheng and others 2006) suggests that conversion of tryptamine to NHT is a rate-limiting step in the tryptamine pathway for IAA biosynthesis. At the present time it is not known how NHT is converted to IAA, although some intermediates have been suggested, including IAOx, IAN, and indole-3-acetaldehyde (Ljung and others 2002; Woodward and Bartel 2005).

Similarity searches indicated that two gene families encode FMO-like proteins in the *Arabidopsis* genome (a dicot), one of them represented by the *YUC* genes (Zhao and others 2001). As shown in Figure 3, a comparable diversification of genes encoding FMO-like proteins is observed in the genome of *Oryza sativa* var. japonica (a monocot). Therefore, it may be speculated that duplications of these genes began before the split of the two main lineages of the angiosperms. Moreover, the *O. sativa* genome has genes that grouped with practically all phylogenetic clades depicted for the *Arabidopsis YUC* gene family (data not shown). This situation suggests that *YUC* genes have acquired a functional diversification that is essential for development or environmental responses. Because multiple biosynthetic pathways may contribute to the regulation of auxin levels, it is also plausible that an additional sophisticated control would be provided by all *Arabidopsis YUC* genes, or at least by those that have been related with IAA production (*YUC1* to *YUC6*), regulating the tryptamine pathway for IAA biosynthesis at the step of NHT synthesis. From this viewpoint, the control of *YUC* gene expression in conjunction with the biochemical properties of each YUC protein would allow a fine tuning of the optimal IAA levels for growth and development. This hypothesis is supported by the high correlation observed between *YUC* mRNAs (Cheng and others 2006) and IAA levels during the development of leaves (Ljung and others 2001) and flowers (Aloni and others 2006) in *Arabidopsis*.

In this study we present evidence that the tomato genome contains at least four paralogous genes of the *YUC* family, the *ToFZY* gene being the best characterized. It may be proposed, based solely on the number of introns and their position in the coding sequence, that *ToFZY* is the ortholog of the petunia *FZY* gene and *Arabidopsis YUC1/YUC4* genes. Nevertheless, the similarities in amino acid sequence, intron sizes, and expression pattern (especially in mature flowers) indicated that *YUC4* is the true ortholog of *ToFZY*. However, from a functional perspective, it appears that *ToFZY* assumes the tasks performed by *Arabidopsis YUC1/YUC2/YUC4/YUC6* genes, which exhibit overlapping expression patterns (Cheng and others 2006). In fact, we did not find any putative tomato ortholog of *Arabidopsis YUC2/YUC6* among the 180,000 ESTs available in the Sol Genomics Network database, whereas we could identify tomato sequences phylogenetically close to the *Arabidopsis YUC3/YUC7* and *YUC5/YUC8/YUC9* clades (Figure 2).

The first study with the loss-of-function *yuc* mutants (Zhao and others 2001) revealed a certain level of functional redundancy in the *Arabidopsis YUC* gene family. Recently, this fact was demonstrated for the gene pairs *YUC1/YUC4* and *YUC2/YUC6* by Cheng and others (2006). These authors also suggested that genetic redundancy of the *YUC* genes is less complex in petunia (also a Solanacea, as is tomato) because the inactivation of the *FZY* gene in petunia led to phenotypes similar to the *yuc1yuc4* double mutant in *Arabidopsis*. This hypothesis seems to be fulfilled in tomato (Figure 2), although a possible example of functional redundancy may be suggested for this species. As discussed by Cheng and others (2006), the two cases of functional redundancy that were experimentally proven in *Arabidopsis* may also be deduced from a phylogenetic tree: YUC1 and YUC4 proteins belong to one clade, whereas YUC2 and YUC6 form another clade. In tomato, the UniGene accessions SGN-U327772/SGN-U330940 and SGN-U329547 encode YUC-like FMOs (partial amino acid sequences) that have a divergence level comparable to that of *Arabidopsis* YUC1/YUC4 or YUC2/YUC6 proteins (Figure 2). Therefore, SGN-U327772 and SGN-U329547 may represent functionally redundant genes in tomato.

Currently, we are determining the nucleotide sequence and gene structure of the three putative tomato paralogs of *ToFZY* to carry out an accurate spatial-temporal expression analysis of the four tomato *YUC*-like genes. Our research

group is interested in the molecular aspects underlying menadione sodium bisulfite effects (MSB, a water-soluble derivate of vitamin K_3), especially on auxin biosynthesis, flower development, and fruit ripening. MSB was found to induce a three- to fourfold higher level of free IAA and the detected increase in tomato fruit yield was correlated with the observed higher level of free IAA (Rama-Rao and others 1985). MSB was also found to accelerate blooming in banana (Borges-Pérez and Fernández-Falcón 1996). Thus, we will include in our expression analyses tomato plants treated with MSB, to verify whether the MSB effect on IAA levels is mediated by the induction of *YUC*-like genes. We also will undertake a detailed search for more tomato *YUC*-like paralogs based on the new conserved motif described in this work, and with the intention of detecting possible orthologs of *Arabidopsis YUC2/YUC6* and *YUC10/YUC11* genes.

Acknowledgments This work was funded by an INVESCAN, S.L. grant (No. 402.01) to the CSIC and supported by a fellowship to MER, a kind gift from the same firm. The authors thank Dr. Giovannoni for kindly providing the clone cTOF (Tomato EST Distribution Center, USDA Plant, Soil, and Nutrition Laboratory). The authors also thank CGM, ABC, and LAD for technical advice on the synthesis of *N*-hydroxyl-tryptamine and HPLC analysis (Instituto de Productos Naturales y Agrobiología, CSIC). They also acknowledge Mrs. Pauline Agnew, who endeavored to edit the English translation of the manuscript.

References

Aloni R, Aloni E, Langhans M, Ullrich CI (2006) Role of auxin in regulating *Arabidopsis* flower development. Planta 223:315–328

Bak S, Nielsen HL, Halkier BA (1998) The presence of CYP79 homologues in glucosinolate-producing plants shows evolutionary conservation of the enzymes in the conversion of amino acid to aldoxime in the biosynthesis of cyanogenic glucosides and glucosinolates. Plant Mol Biol 38:725–734

Bak S, Tax FE, Feldmann KA, Galbraith DW, Feyereisen R (2001) CYP83B1, a cytochrome P450 at the metabolic branch point in auxin and indole glucosinolate biosynthesis in *Arabidopsis*. Plant Cell 13:101–111

Bartel B, LeClere S, Magidin M, Zolman BK (2001) Inputs to the active indole-3-acetic acid pool: de novo synthesis, conjugate hydrolysis, and indole-3-butyric acid ß-oxidation. J Plant Growth Regul 20:198–216

Borges-Pérez A, Fernández-Falcón MJ (1996) Utilization of compositions which contain menadione for stimulation of plant metabolism in order to induce their resistance to pathogen and pest and/or accelerate their blooming. European Patent WO 96/28026

Cashman JR (2002) Human and plant flavin-containing monooxygenase *N*-oxygenation of amines: detoxification vs. bioactivation. Drug Metab Rev 34:513–521

Cheng Y, Dai X, Zhao Y (2006) Auxin biosynthesis by the YUCCA flavin monooxygenases controls the formation of floral organs and vascular tissues in *Arabidopsis*. Genes Dev 20:1790–1799

Cohen JD, Slovin JP, Hendrickson AM (2003) Two genetically discrete pathways convert tryptophan to auxin: more redundancy in auxin biosynthesis. Trends Plant Sci 8:197–199

Cooney TP, Nonhebel HM (1991) Biosynthesis of indole-3-acetic acid in tomato shoots: Measurement, mass-spectral identification and incorporation of ^2H from ^2H_2O into indole-3-acetic acid, D- and L-tryptophan, indole-3-pyruvate and tryptamine. Planta 184:368–376

Dym O, Eisenberg D (2001) Sequence-structure analysis of FAD-containing proteins. Protein Sci 10:1712–1728

Epstein E, Cohen JD, Slovin JP (2002) The biosynthetic pathway for indole-3-acetic acid changes during tomato fruit development. Plant Growth Regul 38:15–20

Gibson RA, Scheider EA, Wightman F (1972) Biosynthesis and metabolism of indol-3yl-acetic acid. II. In vivo experiments with ^{14}C-labelled precursors of IAA, in tomato and barley shoots. J Exp Bot 23:381–399

Goddijn OJM, de Kam RJ, Zanetti A, Schilperoort RA, Hoge HC (1992) Auxin rapidly down-regulates transcription of the tryptophan decarboxylase gene from *Catharanthus roseus*. Plant Mol Biol 18:1113–1120

Hagemann TL, Kwan SP (1997) SeqEd: Manipulation of sequence data and chromatograms from the ABI DNA sequencer analysis files. Methods Mol Biol 70:55–63

Halkier BA, Du L (1997) The biosynthesis of glucosinolates. Trends Plant Sci 2:425–431

Hermkens PHH, Van Maarseveen JH, Ottenheijm HCJ, Kruse CG, Scheeren HW (1990) Intramolecular Pictet-Spengler reaction of N-alkoxytryptamines. 3. Stereoselective synthesis of (-)-debromoeudistomin L and (-)-O-methyldebromoeudistomin E and their stereoisomers. J Org Chem 55:3998–4006

Hull AK, Vij R, Celenza JL (2000) *Arabidopsis* cytochrome P450s that catalyze the first step of tryptophan-dependent indole-3-acetic acid biosynthesis. Proc Natl Acad Sci U S A 97:2379–2384

Kumar S, Tamura K, Nei M (2004) MEGA3: Integrated software for molecular evolutionary genetics analysis and sequence alignment. Brief Bioinform 5:150–163

Laemmli UK (1970) Cleavage of structural proteins during the assembly of the head of bacteriophage T4. Nature 318:78–80

Ljung K, Bhalerao RP, Sandberg G (2001) Sites and homeostatic control of auxin biosynthesis in *Arabidopsis* during vegetative growth. Plant J 28:465–474

Ljung K, Hull AK, Kowalczyk M, Marchant A, Celenza J, et al. (2002) Biosynthesis, conjugation, catabolism and homeostasis of indole-3-acetic acid in *Arabidopsis thaliana*. Plant Mol Biol 50:309–332

Mikkelsen MD, Hansen CH, Wittstock U, Halkier BA (2000) Cytochrome P450 CYP79B2 from *Arabidopsis* catalyzes the conversion of tryptophan to indole-3-acetaldoxime, a precursor of indole glucosinolates and indole-3-acetic acid. J Biol Chem 275:33712–33717

Rama-Rao AV, Ravichandran K, David SB, Ranade S (1985) Menadione sodium bisulphite: a promising plant growth regulator. Plant Growth Regul 3:111–118

Ribnicky DM, Cohen JD, Hu W-S, Cooke TJ (2002) An auxin surge following fertilization in carrots: a mechanism for regulating plant totipotency. Planta 214:505–509

Songstad DD, de Luca V, Brisson N, Kurz WGW, Neisser CL (1990) High levels of tryptamine accumulation in transgenic tobacco expressing tryptophan decarboxylase. Plant Physiol 94:1410–1413

Stehr M, Diekmann H, Smau L, Seth O, Ghisla S, Singh M, Macheroux P (1998) A hydrophobic sequence motif common to N-hydroxylating enzymes. Trends Biochem Sci 23:56–57

Suh JK, Poulsen LL, Ziegler DM, Robertus JD (1996) Molecular cloning and kinetic characterization of a flavin-containing momooxygenase fron *Saccharomyces cerevisiae*. Arch Biochem Biophys 336:268–274

Sztein AE, Ilic N, Cohen JD, Cooke TJ (2002) Indole-3-acetic acid biosynthesis in isolated axes from germinating bean seeds: the effect of wounding on the biosynthetic pathway. Plant Growth Regul 36:201–207

Tobeña-Santamaria R, Bliek M, Ljung K, Sandberg G, Mol JNM, Souer E, Koes R (2002) FLOOZY of petunia is a flavin monooxygenase-like protein required for the specification of leaf and flower architecture. Genes Dev 16:753–763

Woodward AW, Bartel B (2005) Auxin: regulation, action and interaction. Ann Bot 95:707–735

Woodward C, Bemis SM, Hill EJ, Sawa S, Koshiba T, Torii KU (2005) Interaction of auxin and ERECTA in elaborating *Arabidopsis* inflorescence architecture revealed by activation tagging of a new member of the YUCCA family putative flavin monooxygenases. Plant Physiol 139:192–203

Yamada H, Kawate T, Matsumizu M, Nishida A, Yamaguchi K, Nakagawa M (1998) Chiral Lewis acid-mediated enantioselective Pictet-Spengler reaction of N-hydroxyl-tryptamine with aldehydes. J Org Chem 63:6348–6354

Zhang M, Robertus JD (2002) Molecular cloning and characterization of a full-length flavin-dependent monooxygenase from yeast. Arch Biochem Biophys 403:277–283

Zhao Y, Christensen SK, Fankhauser C, Cashman JR, Cohen JD, Weigel D, Chory J (2001) A role for flavin monooxygenase-like enzymes in auxin biosynthesis. Science 291:306–309

Zhao Y, Hull AK, Gupta NR, Goss KA, Alonso, Eckeer JR, Normanly J, Chory J, Celenza JL (2002) Trp-dependent auxin biosynthesis in *Arabidopsis* involvement of cytochrome P450s CYP79B2 and CYP79B3. Genes Dev 16:3100–3112